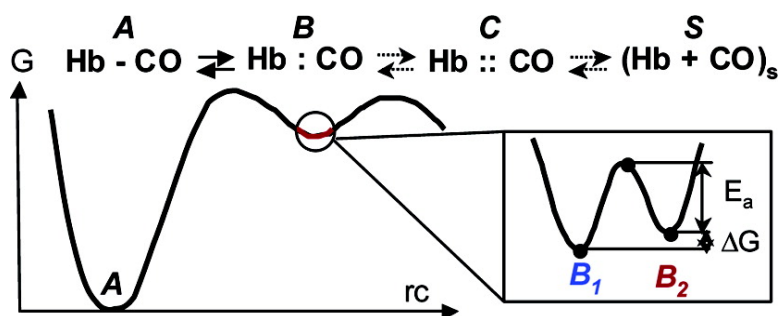


## Picosecond Dynamics of Ligand Interconversion in the Primary Docking Site of Heme Proteins

Seongheun Kim, and Manho Lim

*J. Am. Chem. Soc.*, **2005**, 127 (16), 5786-5787 • DOI: 10.1021/ja050734h • Publication Date (Web): 29 March 2005

Downloaded from <http://pubs.acs.org> on March 25, 2009



### More About This Article

Additional resources and features associated with this article are available within the HTML version:

- Supporting Information
- Links to the 2 articles that cite this article, as of the time of this article download
- Access to high resolution figures
- Links to articles and content related to this article
- Copyright permission to reproduce figures and/or text from this article

[View the Full Text HTML](#)

## Picosecond Dynamics of Ligand Interconversion in the Primary Docking Site of Heme Proteins

Seongheun Kim and Manho Lim\*

*Department of Chemistry, Pusan National University, Busan 609-735 Korea*

Received February 4, 2005; E-mail: mhlum@pusan.ac.kr

Many chemical reactions in proteins are complex, involving multiple intermediate states along the reaction pathway.<sup>1</sup> Probing the intermediates in detail is essential to understand the reaction mechanism in such complex systems.

Ligand binding in heme proteins such as hemoglobin (Hb) and myoglobin (Mb) has long served as a biological model reaction.<sup>2,3</sup> Three decades ago, Frauenfelder and co-workers showed that ligand binding to Mb involves multiple intermediates along the reaction pathway.<sup>2</sup> Only recently have their structural details been characterized.<sup>4–9</sup> Femtosecond IR experiments of photolyzed MbCO at ambient temperature showed that CO becomes temporarily trapped in a nearby ligand docking site *B* before escaping into the surrounding solvent.<sup>7,8</sup> Low-temperature and time-resolved crystal structures of photolyzed MbCO revealed that site *B* is on top of the heme group about 2 Å from the active binding site,<sup>4,5</sup> which is consistent with a location suggested by molecular dynamics (MD) simulations.<sup>6</sup> Secondary docking sites, where ligands migrate as they escape toward solvent, have also been characterized.<sup>5,10</sup> The presence of highly conserved amino acid residues surrounding site *B* in mammalian Hb and Mb indicates that the docking site is functionally important. It has been suggested that site *B* serves as a station mediating the passage of ligand to and from the active binding site, thereby modulating ligand-binding activity.<sup>8</sup> To elucidate how the docking site mediates ligand transport, it is crucial to characterize the free energy surface of the primary docking site under physiological conditions. IR spectroscopy has shown two distinct stretch bands for CO in the *B* state of Hb and Mb.<sup>7,11</sup> Those bands, denoted *B*<sub>1</sub> and *B*<sub>2</sub>, arise from two opposite orientations of CO.<sup>7,8</sup> While the *B* states have been well-characterized, the detailed dynamical information of *B*-state interconversion under physiological conditions has not yet been obtained. Here we use femtosecond IR spectroscopy to probe CO photolyzed from HbCO and MbCO and characterize the equilibration of the two spectral bands. Interconversion rates between the two states were obtained from the time evolution of the fractional population of each band, from which a free energy surface of the docking site was deduced. By comparing Hb and Mb, we explored the effect of quaternary packing of Hb on the ligand dynamics in the docking site.

Figure 1 shows representative time-resolved mid-IR absorption spectra of CO photolyzed from HbCO and MbCO in D<sub>2</sub>O at 283 K.<sup>12</sup> Spectra of MbCO are similar to those of HbCO, but are modestly broader. The two positive-going features correspond to CO located in the primary docking site with opposite orientations.<sup>7,8,11,12</sup> To characterize the spectral evolution, the absorption features were fit to two evolving bands with each band modeled with a sum of two Gaussians on a cubic polynomial background.<sup>12,13</sup> Initial growth of the total integrated area, occurring with a time constant of 1.1 ± 0.1 ps, arises from protein rearrangement that constrains the orientation of docked CO after photolysis.<sup>8</sup> Because escape of CO from the heme pocket and geminate rebinding of

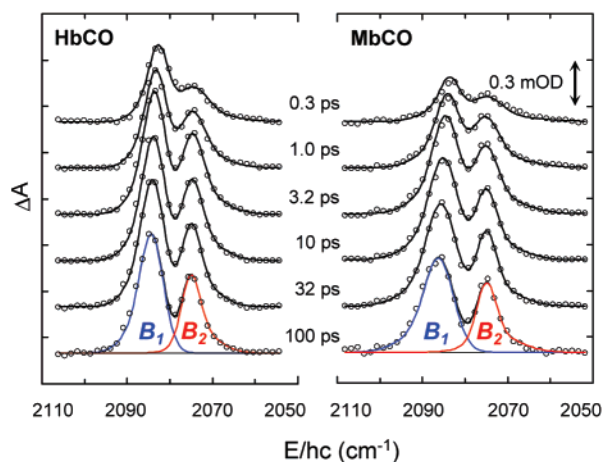


**Figure 1.** Representative time-resolved vibrational spectra of <sup>13</sup>CO photolyzed from Hb<sup>13</sup>CO and Mb<sup>13</sup>CO in D<sub>2</sub>O at 283 K. The data (○) are fit to two evolving bands (*B*<sub>1</sub> and *B*<sub>2</sub>), and each band is modeled as a sum of two Gaussians (—).<sup>12</sup> For clarity, the cubic polynomial background and small hot bands have been subtracted from the measured spectra.<sup>7,8,12</sup> The spectrum at 100 ps is decomposed into two bands. Spectra are offset to avoid overlap.

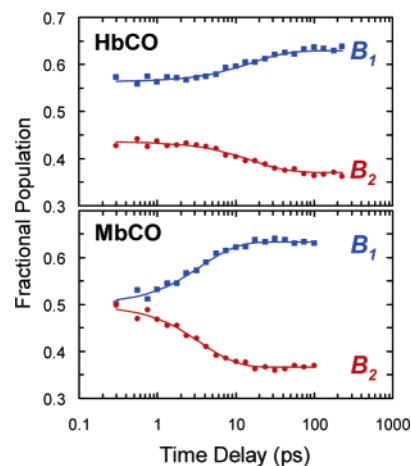


**Figure 2.** Time evolution of the fractional population of each band of photolyzed HbCO and MbCO. The data (■, ●) are well-reproduced by the fit to the relaxation kinetics model (—) described in the text.

CO to Hb and Mb are much slower than 100 ps,<sup>15</sup> the time window of the present experiment, the magnitude of the total integrated area is expected to be maintained after the initial growth, as is the case here.

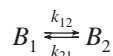
While the total integrated area grows quickly and remains constant, the individual band areas evolve in time, suggesting that the two bands interconvert with each other. Figure 2 shows the time-dependent fractional population of each *B* state from HbCO

**Table 1.** Least-Squares Fit Parameters Obtained by Modeling the Fractional Population in Figure 2

	$1/k_{12}$ (ps)	$1/k_{21}$ (ps)	$f_1(0)$	$\Delta G^a$ (kJ/mol)
HbCO	$43 \pm 2$	$26 \pm 1$	$0.56 \pm 0.02$	$1.18 \pm 0.02$
MbCO	$10 \pm 0.5$	$6 \pm 0.4$	$0.5 \pm 0.02$	$1.20 \pm 0.04$

<sup>a</sup>  $\Delta G = G(B_2) - G(B_1)$  (see text).

and MbCO. The nascent distribution of photoproduct in each state is not in thermal equilibrium, but approaches equilibrium according to the following rate scheme:<sup>16</sup>



The time-dependent fractional population of the  $B_1$  state,  $f_1(t)$ , is given by

$$f_1(t) = k_{21}/k + [f_1(0) - k_{21}/k] \exp(-kt)$$

where  $k = k_{12} + k_{21}$ . Interestingly, the equilibrium population ratio,  $B_1/B_2$ , is the same for Hb and Mb, which is  $1.66 \pm 0.03$  (calculated by  $k_{21}/k_{12}$  in Table 1). Thus, the free energy of  $B_1$  is  $1.19 \pm 0.04$  kJ/mol lower than that of  $B_2$  in both proteins. The fact that  $B_1$  and  $B_2$  are interconvertible on the picosecond time scale confirms that these two states indeed correspond to CO in different states in the same protein molecule. Interconversion between the two states requires end-to-end rotational motion.<sup>7–9</sup> Because the attempt frequency for crossing the barrier can be no faster than the inverse time required for gas-phase CO to rotate  $90^\circ$ , which is  $(0.25 \text{ ps})^{-1}$  at 283 K,<sup>7</sup> the rotational barrier from  $B_2$  to  $B_1$  can be estimated to be  $<11$  kJ/mol in Hb and  $<7.5$  kJ/mol in Mb, which is consistent with 6–20 kJ/mol for Hb and Mb at 283 K, estimated using simple cosine potential,<sup>7</sup> and 3–4 kJ/mol for Mb at 5.5 K.<sup>11</sup>

The nascent yield of  $B_1$  after photolysis is slightly higher in Hb than that in Mb. Assuming that the departing ligand has the same kinetic energy in both Mb and Hb and assuming that  $B_2$  is located slightly farther away from the binding site than  $B_1$ ,<sup>7</sup> one can argue that the tighter side chain packing in Hb reduces the yield of nascent CO in the more distant  $B_2$  site. Conformational relaxation of the protein after photolysis is nonexponential and extends beyond 100 ps; thus, the structural rearrangement of the docking site is not expected to be complete by 100 ps. However, exponential relaxation of the fractional population of two states, as expected in an equilibrating system, suggests that the barrier to interconversion is quickly established and is negligibly affected by slow conformational relaxation. The equilibrium constant between the two  $B$  states in Hb is the same as that of Mb, suggesting that highly conserved amino acid residues surrounding the primary docking site result in the same free energy difference between the two ligand orientations in the proteins. However, slower interconversion rates in Hb imply that the quaternary contact contributes to a higher interconversion barrier in the pocket of Hb. The detailed origins of the interconversion barrier and its difference in Hb and Mb are not yet known, but may be accessible to MD simulations. The accurate intercon-

version rates of both Hb and Mb can be used to refine computer simulations, which could in turn provide a detailed mechanistic picture of ligand binding in heme proteins.

**Acknowledgment.** This work was supported by grants from the Korea Science and Engineering foundation through the Center for Integrated Molecular Systems (POSTECH).

**Supporting Information Available:** Experimental procedures. This material is available free of charge via the Internet at <http://pubs.acs.org>.

## References

- (1) Frauenfelder, H.; Deisenhofer, J.; Wolyne, P. *Simplicity and Complexity in Proteins and Nucleic Acids*; Dahlem University Press: Berlin, 1999.
- (2) Austin, R. H.; Beeson, K. W.; Eisenstein, L.; Frauenfelder, H.; Gunsalus, I. C. *Biochemistry* **1975**, *14*, 5355–5373.
- (3) (a) Tian, W. D.; Sage, J. T.; Champion, P. M. *J. Mol. Biol.* **1993**, *233*, 155–166. (b) Springer, B. A.; Sliagar, S. G.; Olson, J. S.; Phillips, G. N., Jr. *Chem. Rev.* **1994**, *94*, 699–714. (c) Parak, F. G.; Nienhaus, G. U. *ChemPhysChem* **2002**, *3*, 249–254.
- (4) (a) Schlichting, I.; Berendzen, J.; Phillips, G. N., Jr.; Sweet, R. M. *Nature* **1994**, *371*, 808–812. (b) Teng, T. Y.; Srajer, V.; Moffat, K. *Nat. Struct. Biol.* **1994**, *1*, 701–705. (c) Hartmann, H.; Zinser, S.; Kominos, P.; Schneider, R. T.; Nienhaus, G. U.; Parak, F. *Proc. Natl. Acad. Sci. U.S.A.* **1996**, *93*, 7013–7016. (d) Srajer, V.; Teng, T.-y.; Ursby, T.; Pradervand, C.; Ren, Z.; Adachi, S.-i.; Schildkamp, W.; Bourgeois, D.; Wulff, M.; Moffat, K. *Science* **1996**, *274*, 1726–1729. (e) Srajer, V.; Ren, Z.; Teng, T.-Y.; Schmidt, M.; Ursby, T.; Bourgeois, D.; Pradervand, C.; Schildkamp, W.; Wulff, M.; Moffat, K. *Biochemistry* **2001**, *40*, 13802–13815. (f) Adachi, S.; Park, S. Y.; Tame, J. R. H.; Shiro, Y.; Shibayama, N. *Proc. Natl. Acad. Sci. U.S.A.* **2003**, *100*, 7039–7044.
- (5) (a) Chu, K.; Vojtechovsky, J.; McMahon, B. H.; Sweet, R. M.; Berendzen, J.; Schlichting, I. *Nature* **2000**, *403*, 921–923. (b) Schotte, F.; Soman, J.; Olson, J. S.; Wulff, M.; Anfirud, P. A. *J. Struct. Biol.* **2004**, *147*, 235–246.
- (6) (a) Straub, J. E.; Karplus, M. *Chem. Phys.* **1991**, *158*, 221–248. (b) Carlson, M. L.; Regan, R.; Elber, R.; Li, H.; Phillips, G. N., Jr.; Olson, J. S.; Gibson, Q. H. *Biochemistry* **1994**, *33*, 10597–10606. (c) Vitkup, D.; Petsko, G. A.; Karplus, M. *Nat. Struct. Biol.* **1997**, *4*, 202–208. (d) Ma, J.; Huo, S.; Straub, J. E. *J. Am. Chem. Soc.* **1997**, *119*, 2541–2551. (e) Meller, J.; Elber, R. *Biophys. J.* **1998**, *74*, 789–802. (f) Nutt, D. R.; Meuwly, M. *Biophys. J.* **2003**, *85*, 3612–3623.
- (7) (a) Lim, M.; Jackson, T. A.; Anfirud, P. A. *J. Chem. Phys.* **1995**, *102*, 4355–4366. (b) Lim, M.; Jackson, T. A.; Anfirud, P. A. *J. Am. Chem. Soc.* **2004**, *126*, 7946–7957.
- (8) Lim, M.; Jackson, T. A.; Anfirud, P. A. *Nat. Struct. Biol.* **1997**, *4*, 209–214.
- (9) Nienhaus, K.; Olson, J. S.; Franzen, S.; Nienhaus, G. U. *J. Am. Chem. Soc.* **2005**, *127*, 40–41.
- (10) Kriegl, J. M.; Nienhaus, K.; Deng, P.; Fuchs, J.; Nienhaus, G. U. *Proc. Natl. Acad. Sci. U.S.A.* **2003**, *100*, 7069–7074.
- (11) Alben, J. O.; Beece, D.; Bowne, S. F.; Doster, W.; Eisenstein, L.; Frauenfelder, H.; Good, D.; McDonald, J. D.; Marden, M. C.; Mo, P. P.; Reinisch, L.; Reynolds, A. H.; Shyamsunder, E.; Yue, K. T. *Proc. Natl. Acad. Sci. U.S.A.* **1982**, *79*, 3744–3748.
- (12) Kim, S.; Heo, J.; Lim, M. *Bull. Kor. Chem. Soc.* **2005**, *26*, 151–156. Experimental details are given in this reference.
- (13) The cubic polynomial represents a small but broad absorption over the entire spectral range, which arises from vibrational heating of the chromophore by the pump pulse.<sup>7,14</sup> Small hot bands, resulting from vibrationally excited CO (about 6% of the total population), were modeled as red-shifted replicas of the two  $B$  states.<sup>7</sup> The first moments of the bands shift nonexponentially, which has been attributed to conformational relaxation of protein after photolysis.<sup>8,12</sup>
- (14) (a) Anfirud, P. A.; Han, C.; Hochstrasser, R. M. *Proc. Natl. Acad. Sci. U.S.A.* **1989**, *86*, 8387–8391. (b) Lian, T.; Locke, B.; Kholodenko, Y.; Hochstrasser, R. M. *J. Phys. Chem.* **1994**, *98*, 11648–11656.
- (15) (a) Henry, E. R.; Sommer, J. H.; Hofrichter, J.; Eaton, W. A. *J. Mol. Biol.* **1983**, *166*, 443–451. (b) Murray, L. P.; Hofrichter, J.; Henry, E. R.; Eaton, W. A. *Biophys. Chem.* **1988**, *29*, 63–76.
- (16) In the first 100 ps, two states interconvert without geminate recombination and ligand escape. Consequently, other states (bound, secondary pockets, and solvent) need not be included in this analysis. The fact that the total integrated area remains constant after the initial growth indicates that the population of CO in each state is proportional to its integrated absorbance.

JA050734H